remote sensing

MDPI

Article

Identifying and monitoring volcanic activity in Europe using satellite data

Catarina Alonso [1,2], Rita Durão [1,3] and Célia M. Gouveia [1,4,*]

[1] Instituto Português do Mar e da Atmosfera, I.P., Rua C do Aeroporto, 1749-077 Lisboa, Portugal celia.gouveia@ipma.pt; joao.p.martins@ipma.pt; rita.durao@ipma.pt; isabel.trigo@ipma.pt
[2] Centre for the Research and Technology of Agroenvironmental and Biological Sciences (CITAB), Universidade de Trás-os-Montes e Alto Douro, Vila Real, Portugal
[4] Centro de Recursos Naturais e Ambiente, Instituto Superior Técnico, Universidade de Lisboa, 1049-001, Lisboa, Portugal.
[3] Instituto Dom Luiz, Faculdade de Ciências, Universidade de Lisboa, 1749-016 Lisboa, Portugal; acrusso@fc.ul.pt;
* Correspondence: celia.gouveia@ipma.pt; Tel.: +351 21 844 70 00

Abstract: Volcano eruption monitoring is crucial to better understanding volcanoes dynamics, namely near real-time monitoring of eruption start, end and duration. Eruptions monitoring allows hazard assessment, eruption forecasting and warnings, and also risk mitigation during unrest periods to enhance public safety and reduce losses from volcanic events. The near real-time Fire Radiative Power (FRP) product retrieved using information from SEVIRI sensor onboard of Meteosat Second Generation (MSG) satellite is used to identify and monitor the volcanic activity at the Pan European level, namely the Mount Etna and Cumbre Vieja eruptions occurred during 2021. The FRP is designed to record information on the location, timing, and fire radiative power output of wildfires. Measuring FRP from SEVIRI/MSG and integrating it over the lifetime of a fire provides an estimate of the total Fire Radiative Energy (FRE) released. FRE has been related to the total amount of pollutant emissions during the volcanic events. Together with the FRP data analysis, SO2 data from Copernicus Atmosphere Monitoring Service (CAMS) is used to assess the relationship between SO2 daily emitted concentrations and the radiative energy released during the volcanic eruptions. Results show that the FRP and FRE data reproduces the amount of energy released and the pollutant concentrations from the volcanic emissions during the considered events. A good agreement between FRP detection and SO_2 atmospheric concentrations was found for the considered eruption occurrences. The adopted methodology can, therefore, be used as a management tool, to help authorities to monitor and to manage resources during ongoing volcanic events.

Keywords: Fire radiative Power; SO2 Concentrations; SEVIRI; CAMS; Mount Etna; Cumbre Vieja

Citation: Alonso, C.; Durão, F.; Last-name, F. Title. *Remote Sens.* **2023**, *14*, x. https://doi.org/10.3390/xxxxx

Academic Editor: Firstname Last-name

Received: date
Accepted: date
Published: date

1. Introduction

During the last 3 decades of the XX century, according to the Global Assessment Report on Disaster Risk Reduction 2022 [1] were reported around 90 to 100 medium and large scale volcanic disasters per year. However, between 2001 and 2020, the number of these events increased to 350 to 500 per year. Nonetheless, some high-exposure volcanoes remain unmonitored, and more than 800 million people live within 100 km of a volcano that could erupt [2].

The monitoring of volcanic activity provides relevant information to better understand the structure and dynamics of volcanoes and is crucial for hazard assessment, eruption forecasting and warnings, as well as risk mitigation during volcanic unrest [3]. During volcanic eruptions, significant amounts of ash particles and gases are injected into

the atmosphere interacting with anthropogenic activities and ecosystems on various levels [4,5]. The lava and magma flows can also cause massive destruction and devastation, overwhelming whole villages, burying key infrastructure, and rendering land unproductive or uninhabitable [6].

Depending on the eruption characteristics (eruptions can be described by a mixed mechanism of simultaneous explosive and effusive phases), ejected materials can reach the troposphere or stratosphere, affecting the global radiative balance and surface temperatures [4,7]. Despite this important role as a natural forcing of the climatic system, volcanic activity also impacts air quality (low levels of air quality) and airspace security (e.g. by reducing visibility) [8]. Therefore, following up on volcanic activity and monitoring volcanic materials (ash and gases) revealed to be of primordial importance, since it is the only way to avoid and mitigate their harmful effects.

Regarding the several volcanic materials released into the atmosphere, SO_2 is the most common gas, with its injected amounts directly linked to the volcano's eruption explosivity [5,8]. Generally, SO_2 concentrations are slowly removed from the emitted plumes, having an important impact on climate through radiative forcing, which could produce either surface cooling or surface warming effects [8-11]. In the troposphere, sulfur compounds accelerate the oxidation of metals, and volcanic sulfate aerosol has been implicated in some aviation incidents [12]. In the stratosphere, volcanic sulfate aerosol can remain for months and even years, depending on the SO_2 injection altitude, total mass loading, latitudes, and dispersion patterns [13, 14]. Moreover, SO_2 exposure may cause negative effects on health and the environment. Namely, short-term exposures to this gas can irritate the eyes, harm the human respiratory system, and make breathing difficult. People with asthma, particularly children, are the most sensitive to these effects due to airway constriction [15]. SO_2 exposure has been also linked to cardiovascular diseases [15]. As well, SO_2 high concentrations have harmful effects on trees and plants, by damaging foliage and decreasing growth. Besides, it can contribute to acid rain which can harm sensitive ecosystems; and by reacting with other compounds in the atmosphere to form fine particles, may also reduce visibility (haze) over affected areas [15,16].

The use of remote sensing data is a useful approach to conveniently assess volcanic activity, allowing early and rapid detection, quantitative characterization, plume tracking and eruption forecasting; and specifically allowing the monitoring of remote inaccessible volcanic areas at different time scales [5,8,17]. Particularly, the evolution of satellites in recent years marked a great advance in the proximal and distal monitoring of volcanic eruptions in areas with scarce instrumentation and/or difficult access [4,18].

Geostationary satellites offer a unique opportunity to follow up, in near real-time, the entire evolution of volcanic eruptions, expanding monitoring capabilities on an hourly basis, with a time step of 10 or 15 minutes [4,19,20]. By monitoring near-real-time a volcanic eruption, geostationary satellites can help to reduce risks to the population and local air traffic, as well as to detect different types of volcanic activity [5,17]. Additionally, sensing-based tools are less cost-effectively when compared to ground-based monitoring instrumentation, which is more vulnerable to destruction by volcanic activity, theft, or burns [18,21].

In the last years, some volcanoes have been active over Europe, namely the Mount Etna in Italy, and the Cumbre Vieja in the Canary Islands [22-26]. In the present work, geostationary satellite data is used to show its ability to identify the eruption start and end, in near real-time, as well as to monitor the volcanic activity and assess it intensity of these two volcanic events. In order to detect the hotspots and to assess the intensity of Mount Etna and Cumbre Vieja eruptions, the near real-time Fire Radiative Power Pixel (FRP) from the product retrieved using information from SEVIRI sensor onboard of Meteosat Second Generation (MSG) satellite is used. The FRP was originally designed to record information on the location, timing and fire radiative power emitted by wildfires (in MWatts), detected every 15 minutes across the full MSG disk, at the native spatial resolution of the Spinning Enhanced Visible and InfraRed Imager (SEVIRI) sensor [27,28].

Since the radiative power emitted by fires can be related to the production of smoke during combustion [29], the potential of using FRP as a proxy of volcanic gas emissions, namely SO_2, is also evaluated in this work. Hence, the concentration of the SO_2 released in volcano area surroundings was characterized for each event, to assess the respective spatio-temporal patterns, based on data provided by the Copernicus Atmosphere Monitoring Service (CAMS). Finally, the relationship between SO_2 daily emitted concentrations and the radiative energy released during eruptions was assessed for both volcanic events.

2. Data and Methods

2.1. Study Area

Mount Etna is a basaltic volcano located on the eastern coast of Sicily, Italy, and has had eruptions that date back 3,500 years [30,31,32]. It is one of the most active volcanoes in the world [32], representing a potential hazard for about 600 000 people living on its slopes, as well as hundreds of thousands of tourists who visit the volcano yearly [16]. The volcanic activity of Mount Etna, which can be both explosive and effusive, has been particularly active and intense in the last 30 years [22-25,33].

The Cumbre Vieja is historically the most active volcano in the Canary Islands in Spain. After 50 years of sleeping, the Cumbre Vieja volcano woke up with an eruptive episode on 19th September that lasted until 13th December 2021 [26]. For three months, the Cumbre Vieja eruption, of Strombolian type, produced lava fountains and flows and injected ash and gases into the atmosphere. The characteristics of this eruptive event forced the evacuation of about 6400 residents and destroyed infrastructure worth more than 400 million euros [26].

The methodology to identify and monitor volcanic eruption in European Island during 2021 eruptive events was performed over the volcanic surrounding areas: [14.4E-15.6E; 37.4N-38.2N] for Mount Etna, and [18.2W-17.4W; 28.4N-28.8N] for Cumbre Vieja. The areas correspond to the areas inside the dashed boxes in Figure 1.

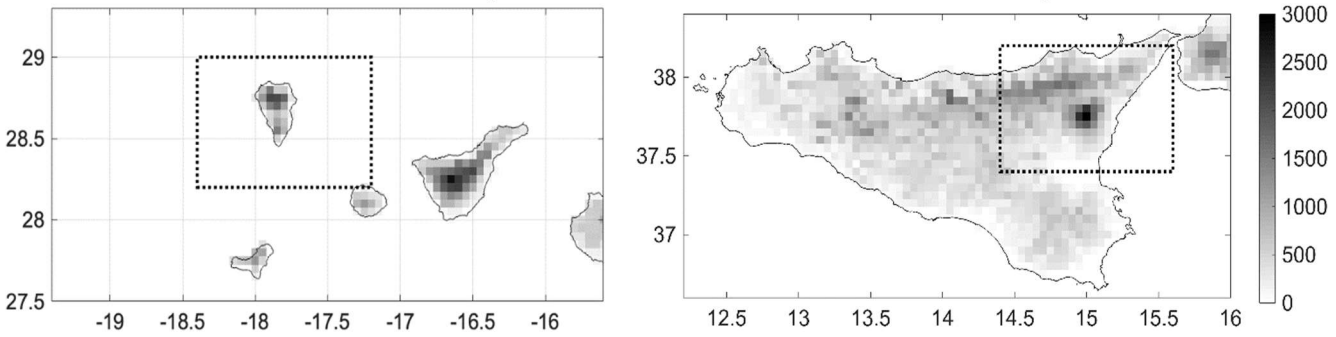

Figure 1. Study Area inside the dashed box: Mount Etna (right panel) and Cumbre Vieja (left panel).

2.2. Data

The FRP is derived from the SEVIRI instruments, on board the MSG geostationary satellite, delivered in near real-time, since 2004, by the EUMETSAT Land Surface Analysis Satellite Applications Facility (LSA-SAF).

FRP is disseminated for the full spatiotemporal resolution of the SEVIRI imager, with a 3 km spatial sampling distance at the sub-satellite point (decreasing away from the West African sub-satellite point), with a temporal resolution of 15 minutes. The FRP of an active fire pixel is expressed in megawatts (MW) and represents the amount of radiant heat energy emitted, per time unit, by the burning vegetation and/or organic soils present within that pixel. FRP quantifies the release rate of radiant energy by a fire, over all wavelengths based on Stefan's Law, which relates total emitted radiance over all

wavelengths (i.e., the Fire Radiative Power) to emitter temperature [29]. Likewise, the thermal emission of an active volcanic surface relates directly to the radiative power of the emitter at a specific time. The FRP algorithm confidently detects active fire pixels whose FRP exceeds 30 MW [34], and can discriminate actively burning fires covering down to 10^{-4} of a pixel, being, therefore, more sensitive to fire than other algorithms that are used in many active fire products, widely exploited [29]. A full description of the FRP/MSG operational algorithm is fully described by Wooster et al. (2015).

By definition the FRP algorithm assumes that fire temperature ranges from 665 K to 1365 K [29]; on the other hand, lava and magma temperatures range from 1073 K to 1473 K [36]. For example, in fires case studies, FRP is used as a proxy of fireline intensity, helping to develop mitigation strategies [37,38], in the case of volcanic events, it is expected that it can be used to understand eruption dynamics and the direction of lava flow, to assess dangerous areas and issue evacuation alerts.

In the normal state of moderate and persistent activity of Mount Etna, the magma extrudes at a nearly constant temperature of 1353 K, and during stronger paroxysmal eruptions the magma temperature is higher (~1398 K) [39]. For the Cumbre Vieja eruption in 2021, it is estimated that the magma temperatures ranged approximately from 1373K to 1433K [40]. As these temperature values are included in the temperature spectrum detected by the FRP algorithm, it follows that this product can be properly used to detect the radiative power emitted by volcanoes.

The SO_2 concentrations were obtained through the global atmospheric composition forecasts (GACF) data from Copernicus Atmosphere Monitoring Service (CAMS), a component of the European Earth Observation program Copernicus. GACF are produced twice a day, of more than 50 chemical species and seven different types of aerosols. For each forecast, the initial conditions are obtained by combining a previous forecast with current satellite observations through data assimilation, providing a complete and consistent dataset that enables estimations at sites where observation coverage is poor or for atmospheric pollutants for which no direct observations are available (https://ads.atmosphere.copernicus.eu). GACF are available on a regular 0.44° x 0.44° resolution grid, from 2015 up to now, on hourly resolution.

For the present study, SO_2 data, namely the total column sulphur dioxide, was selected at the surface level, being used to assess spatial and temporal patterns of emitted concentrations into the atmosphere during Mount Etna and Cumbre Vieja eruptions in 2021, over the defined study areas above.

2.3. Methods

Integrating FRP obtained from SEVIRI/MSG with the temporal resolution of 15 minutes over the lifetime of fire is possible to estimate the total Fire Radiative Energy (FRE) released during the event. The adopted methodology relies on the fact that released Fire Radiative Energy (FRE) is proportional to the amount of biomass consumed and therefore to the intensity of the eruption, computed using the accumulated FRP of each event [39,40].

By definition the FRP algorithm assumes that fire temperature ranges from 665 K to 1365 K [29]; on the other hand, lava and magma temperatures ranging from 1073 K to 1473 K [36]. For example, in fires case studies, FRP is used as a proxy of fireline intensity, helping to develop mitigation strategies [27,28], in the case of volcanic events, it is expected that it can be used to understand eruption dynamics and the direction of lava flow, to assess dangerous areas and issue evacuation alerts. In this work, the FRP was used to identify and analyze the periods of highest activity on Mount Etna and Cumbre Vieja, in terms of emitted radiative energy, and the start and end date of the eruption, respectively.

For each active pixel, the hourly FRP was determined as the accumulated values of each 15 minutes of an hour and, in turn, the daily FRP is the accumulated of the 24 hours. Subsequently, the FRP hourly and daily for the study areas correspond to the hourly and

daily accumulated FRP, of all pixels present in the study areas. The daily FRE was calculated for each volcanic event using the formula by Pinto et al. 2018 [41].

The released daily SO_2 concentration was obtained by the accumulated value of all GACF pixels in the volcanic surrounding areas, previously defined above. Maps of daily SO_2 concentrations for the period of the eruptive events were also produced for the areas of Figure 1. To analyze the temporal evolution of FRP/FRE and SO2 emissions related to the volcano's eruptions the hourly/daily accumulated values of FRP and FRE and SO2 concentration were summed over the boxes defined inside Figure 1.

3. Results

3.1. Volcanic activity in Mount Etna

The periods of volcanic activity for Mount Etna, as obtained using the daily FRP accumulated for the selected box and over the entire year of 2021, are shown in Figure 2. The higher daily values of FRP associated with the moments of greatest volcanic activity occurred during February, April, June, July, and August (Figure 2, upper panel). High activity spanning over several consecutive days is observed during February and July. The bottom panels of Figure 2 show the hourly periods of FRP during these two months, allowing to identify begin of eruptive events and the moments of high explosive activity. The maximum hourly FRP values observed during the analyzed months, occurred on March 4th, at 9 am, reaching a radiative power of about 35 GW and the second maximum occurred on July 4th at 4 pm, with an emitted radiative power of the same magnitude, exceeding 33 GW (Figure 2, bottom panels). High emitted radiative power values are also observed for March 12th and 31st and July 2nd, 7th, 8th and 31st (Figure 2, bottom panels).

The daily FRE accumulated over the selected box considering the Etna Eruption in 2021 is observed in Figure 3 (blue line). The maximum of daily FRE released occurred on March 12th, with a release of 126 TJ. Other relative maxima are observed on March 4th (111TJ), April 1st (102 TJ), and August 9th (105 TJ). It should be stressed that the FRE and FRP maximum values may not occur on the same day, because the maximum FRE corresponds to the day with longer continuous and intense volcanic activity and not to the day of maximum FRP emitted. However, for the period and area under analysis, March 4th was the second day with the highest FRE released, in agreement with the observed in Figure 2. However, in Figure 3 is evident the persistent volcanic activity for several days in February, March, June and July.

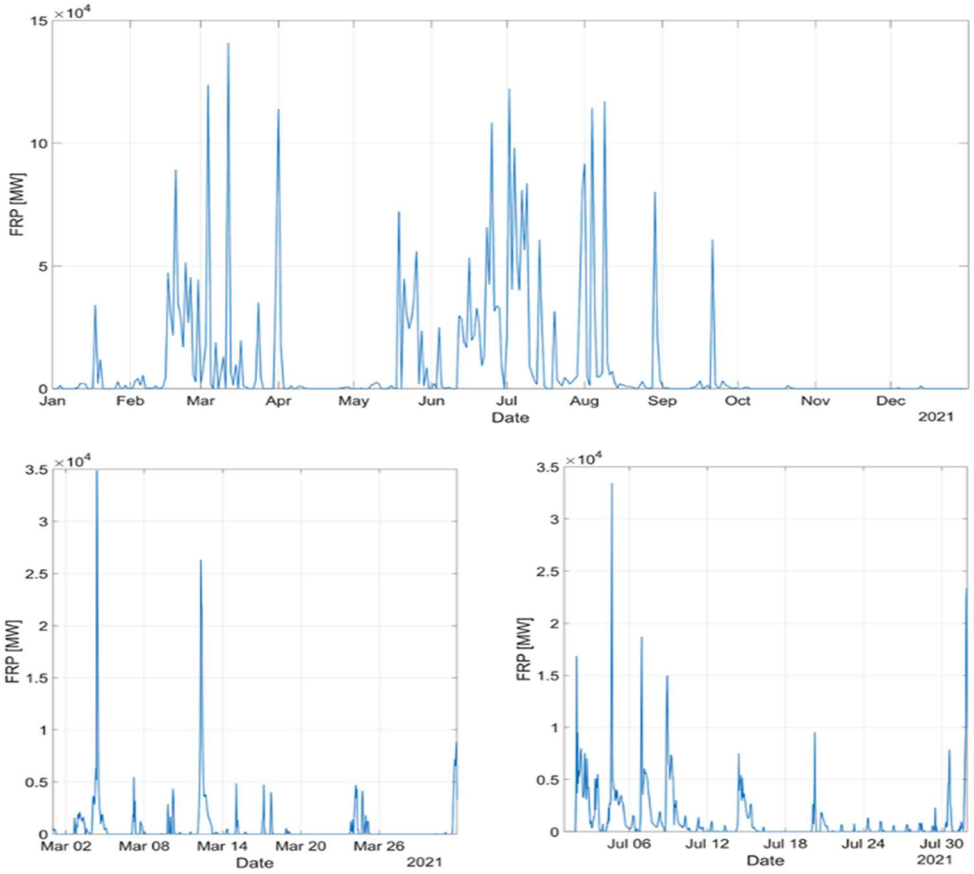

Figure 2. Daily FRP (MW) accumulated over the dashed box for Mount Etna in Figure 1 covering the total period (top panel) and the hourly FRP (MW) for March (left bottom panel) and July (right bottom panel).

The injection of SO_2 into the atmosphere during the Mount Etna eruption months resulted in three distinct peaks of daily maximum SO_2 concentrations, as shown in Figure 3 (orange line). Namely, on February 28th, April 1st, and June 16th, with maximum released concentrations of 1775 μg/m^3, 1823 μg/m^3, and 1820 μg/m^3, respectively (Figure 3, line orange). It should be also noted that, as expected, daily concentrations of SO_2 follow the intensity of the volcanic activity, revealing a similar temporal pattern as the FRE released during the Mount Etna eruption. This behavior pattern is evident on days with FRE higher values, such as March 4th and 12th (111 and 126 TJ), April 1st (102 TJ), and August 9th (105 TJ), where the concentration of SO_2 is higher than 1150 μg/m^3 (Figure 3, blue line).

In order, to better evaluate the impacts of SO_2 emissions over the volcanic-affected areas, FRE and SO_2 values were spatially represented, as can be seen on Figure 4, for two days of maximums of Etna's volcanic activity, March 4th and April 1st. The daily concentrations of SO_2 on April 1st were higher than on March 4th, however, on both days, SO_2 values were above the 300 μg/m^3 over the volcano area. It also should be noted that the higher SO2 concentrations are located in the southeast part of the island, probably related to the movement of the plume to the south associated with the prevalent wind direction of the considered day.

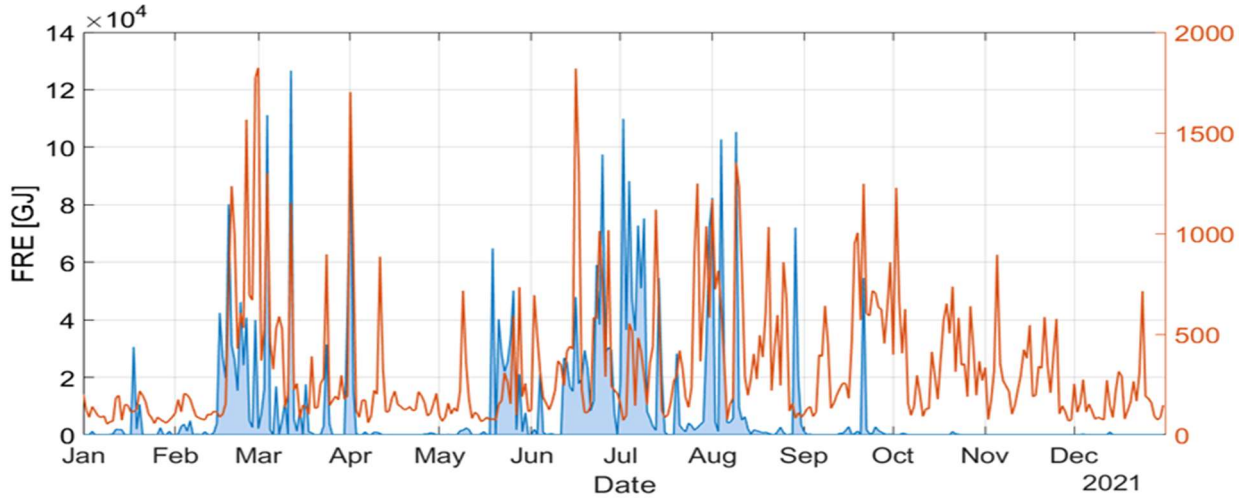

Figure 3. Daily FRE (blue, GJ) and SO_2 (orange, μ/m³ accumulated over the dashed box for Mount Etna in Figure 1.

The area Mount Etna affected by volcanic activity, with respect to energy released, was larger on March 4th (Fig. 3, left panel), however showing lower FRE pixels as the distance to the volcano center increased, potentially related to the faster cooling of the lava, in locals at a greater distance to the center of the volcano. Although FRE values are lower on March 4th (maximum 10.54 TJ) than on April 1st (maximum 18.45 TJ), FRE accumulated in the study area on March 4th is slightly higher (111 TJ) than on April 1st (102 TJ), as on March 4th the eruption covered a greater number of pixels.

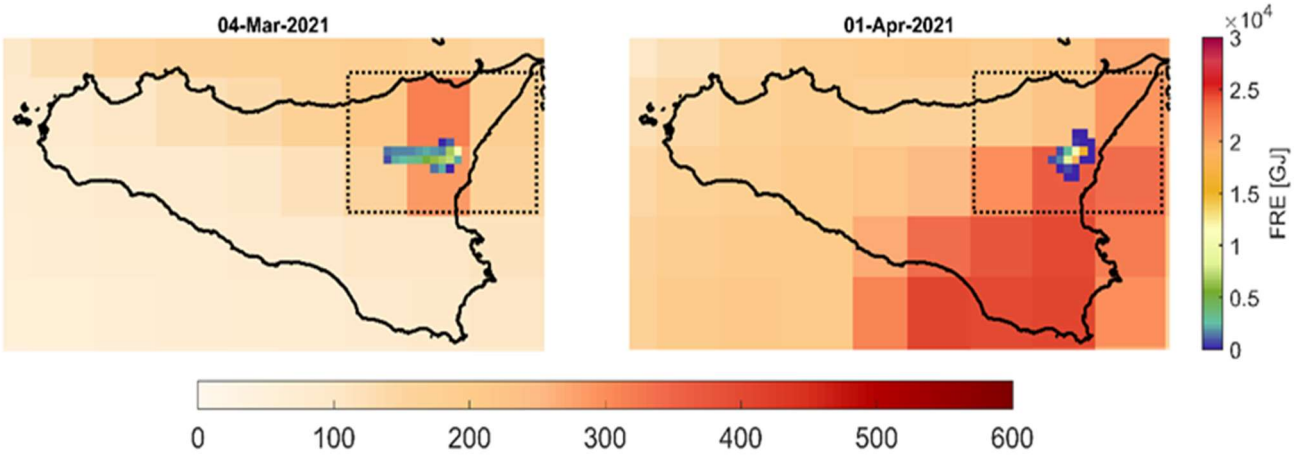

Figure 4. FRE (GJ) and SO_2 (μ/m³) concentration on March 4th (left painel) and FRE and SO_2 concentration on April 1st (right painel). The dashed rectangle represents the area where the accumulated FRP, FRE and SO_2 previously represented were calculated for Mount Etna.

3.2. Volcanic activity in Cumbre Vieja:

The periods of volcanic activity for Cumbre Vieja, as obtained using the daily FRP accumulated for the selected box and over the entire year of 2021, are shown in Figure 5. The Cumbre Vieja volcanic activity began on September 19th and continued until December 13th, presenting the maximum radiative power of around 90 GW on October 2nd and relative maxima on October 16th and 23rd above 40 GW (Figure 5, top panel). The radiative power is low and intermittent between the beginning of November and the first half of December. Figure 5 (bottom panel shows the period of greatest activity of the volcano, from September 28th until October 12th, on an hourly basis. It should be noted that FRP values were above 4 GW several times between October 1st at 6 p.m. and October 3rd at 7

p.m., reaching the maximum value on October 1st at 9 p.m. In addition to that period, values also above 4 GW occurred on September 28th at 7 p.m. and 11 p.m., and on October 4th and 6th at 6 p.m.

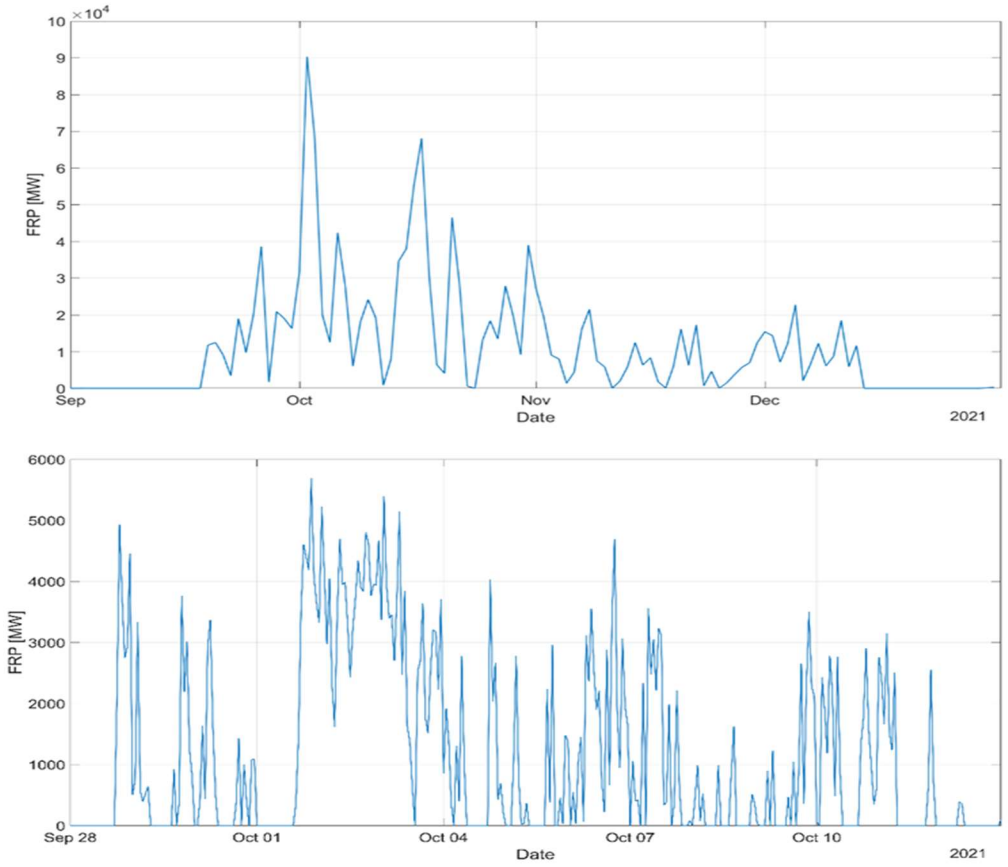

Figure 5. Daily FRP (MW) from September to December (top panel) and hourly FRP (MW) from September 28th to October 12th (bottom panel) for Cumbre Vieja.

The daily FRE accumulated over the selected box considering the Cumbre Vieja in 2021 is observed in Figure 6 (blue line). Intense volcanic activity, as derived from daily accumulated radiative energy released higher than 7 TJ is observed between September 28th and October 28th. It should be noted the FRE maximum value of around 8,1 TJ occurred on October 2nd. A downward trend in FRE values is observed after the beginning of November, achieving negligible values of daily FRE in the second half of December (Figure 6, blue line).

The SO_2 concentrations released into the atmosphere during the Cumbre Vieja activity are also related to the FRE values emitted during the eruption periods, as expected. Both FRE maximum value (8,1 TJ) and SO_2 maximum concentration (3122 $\mu g/m^3$) occurred on October 2nd (Figure 6, orange line), and as the FRE diminished due to the volcano's activity decreasing, the SO_2 concentration also declined after December 15th.

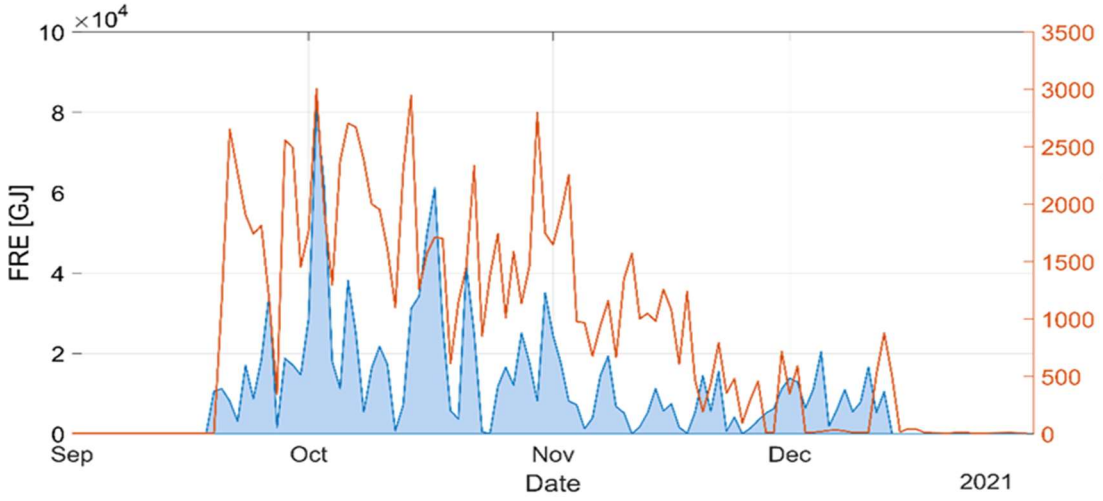

Figure 6. Daily FRE (blue, GJ) and SO2 (orange, μ/m³) for the same area and period for Cumbre Vieja.

Similarly, to the Mount Etna event, two days with high FRP and SO_2 values were identified and spatially represented for the Cumbre Vieja eruption, respectively October 2nd and 17th (Figure 7). Regarding the FRE values at the pixel scale, on October 17th, FRE values (2.7 TJ) were almost the same magnitude as the FRE values released on the 2nd of October (FRE ~ 2,5 TJ). However, on October 2nd more active pixels were detected, making the daily accumulation in the volcano area higher than on October 17th. This behavior is also reinforced by the highest amounts of SO_2 released into the atmosphere on October 2nd, above the 500 μg/m³, whereas the concentrations of SO_2 were below the 300 μg/m³ on October 17th.

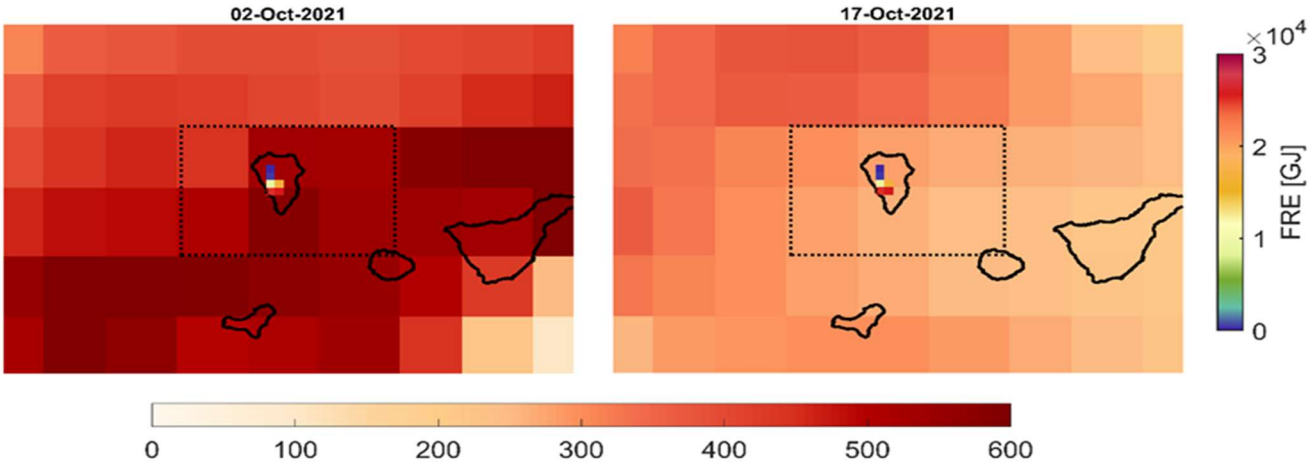

Figure 7. As in Figure 3, but for Cumbre Vieja on a) October 2nd and on b) October 17th 2021.

Comparing the activity of both volcanic events, Mount Etna has hourly FRP values much higher than those reached by Cumbre Vieja. On the other hand, Cumbre Vieja activity was persistently high over a period of consecutive days showing high hourly FRP values continuously recorded. Since the FRE is the cumulative FRP, the maximum FRE reached by each volcanic eruption differs in a scale of only 4 GJ between both. Furthermore, Mount Etna has a higher area of volcanic activity pixels (Figure 4) than Cumbre Vieja (Figure 7), which could also be a reason for the FRE value to be higher for Mount Etna (Figure 3) than for Cumbre Vieja (Figure 4). The different FRP and FRE patterns are probably directly linked to the type of volcanic eruption, which is as well associated with

the amounts of SO_2 released into the atmosphere, as previously shown. However, the analysis of the type of each volcanic eruption is out of the scope of the present work.

4. Discussion

Volcanic eruptions are important natural sources of atmospheric pollutants due to the injection of ash particles and gases – such as carbon dioxide (CO_2), water vapour (H_2O) and sulphur dioxide (SO_2), into the atmosphere [8]. Apart from the climate effects, volcano emissions also have important impacts on air quality and airspace security, being mandatory to monitor it [8], to better assess and anticipate its impacts.

For example, Mount Etna's mean SO_2 flux emitted was equivalent to the total of industrial France (~ 5000 T/day), making it the largest continuous point source of SO_2 globally [41]. On the other hand, when the Cumbre Vieja erupted on September 19th, the SO_2 plumes travelled mainly across Northern Africa and Southern Europe, probably affecting Northern and Western Europe [43]. After, in early October, when the wind direction changed, volcanic plumes were transported over long distances, reaching the Caribbean islands, and decreasing local air quality levels, due to SO_2 huge concentrations, together with a Saharan dust intrusion arrival [42].

According to reports issued by the Global Volcanism Program [43], the maximum FRP and FRE periods coincide with the days of high volcanic activity at Mount Etna and Cumbre Vieja eruptions. Since December 2020, Mount Etna had frequent strombolian explosions of variable intensity, effusive activity, ash emissions, and ashfall [43]. The Istituto Nazionale di Geofisica e Vulcanologia (INGV) reported that a series of paroxysmal events separated by relative calm periods at Mount Etna began on February 16th [44], and those episodes were easily identified from the FRP and FRE patterns, presented on Figure 1. For example, on March 4th, it was the 9th episode, at 8.50 a.m. there was strombolian activity with 300-m-tall lava fountaining and ash plumes rose 11 km above the summit and caused lapilli to fall around the volcano (20 km). This episode agrees with FRP, FRE, and SO_2 values observed and presented in Figures 3 and 4, respectively. On March 31st, there was a strong explosion followed by several clouds of ash, marking the beginning of the 17th episode of lava fountains. Lava fountains continued to be visible during April 1st and the intense strombolian activity produced dense plumes of ash that reached 9 km in and drifted SSW, as is visible in Figure 3, left side. INGV reported three episodes of lava fountaining from June 28th to July 6th [45], the second episode began at 5 p.m. on July 4th, one of the maximum values of FRP identified (Figure 2).

In the Cumbre Vieja event, a fissure eruption began at 2 p.m. on September 19th, with a large explosion that produced a gas-and-ash plume at about 1 km altitude [14]. Once FRP detected the start of the eruption at 7 p.m. instead of 2 p.m. it may be due to the gas-and-ash plume avoiding the satellite sensors to measure exactly the start time of the eruption. Still, the maximum values of FRE and SO_2 concentration released from Cumbre Vieja agrees with the opening of two vents about 600 m NW from the main cone during late September 30th and October 1st; leading to strong volcanic activity on October 2nd, with ash plumes rising to 3-5 km and drifted S [46], as can be seen in Figure 6, a.

The calculation of the accumulated value of the daily FRP, related to the time of each eruption, shows that the amount of energy released by volcanic activity is very high, being in line with the eruption's intensity. Considering that 2000 GJ is the typical daily amount of energy released by a severe fire [39], results show that these volcanic eruptions can release up to 40x to 60x more energy. Moreover, as FRE is defined as the emitted radiant energy released during combustion, it can be linked to the fire's smoke production [47], and consequently, it can be used as a proxy of volcanic emissions into the atmosphere.

The sulfur dioxide emissions affect the balance of the radiative forcing of climate, with several harmful consequences for human health and activities, and ecosystems. Thus, regarding the protection of human health and activities, there are two SO_2 limit values that should not be exceeded, accordingly to the European Air Quality Directive (2008/EC/50) [48]: i) SO_2 hourly mean value may not exceed 350 $\mu g/m^3$ more than 24 times

in a year, and ii) SO_2 daily mean value may not exceed 125 μg/m³ more than 3 times in a year.

Taking this into account, both volcanic emissions considered here, far exceeded the recommended human health thresholds. Namely, the Mount Etna eruption had 79 days over 500 μg/m³, whereas the Cumbre Vieja had 66 days with SO_2 concentrations higher than 500 μg/m³. In accordance with what is known for each eruption, Mount Etna and Cumbre Vieja volcanos are associated with different SO_2 plumes, due to the different eruptive activity and dynamics of each volcano and to different local/regional diffusion processes. These released SO_2 concentrations, are as well in line with the observed FRE values (which can be easily correlated with SO_2 concentrations); corroborating the rationale that FRE can be used as a proxy of volcanic emissions into the atmosphere. Therefore, the proposed monitoring methodology, based on FRP data, shows that is possible to assess potential exceedances of SO_2 threshold levels, allowing issuing several alerts to protect local populations from the adverse consequences of SO_2 high concentrations for human health and activities.

5. Conclusions

Identifying and monitoring volcanic activity on a real-time basis can help to reduce risks to the population and local air traffic, as well as obtain information about the processes and dynamics of volcanic eruptions. Moreover, it can contribute to avoiding their impacts in the short-term (e.g. physical damage) and long-term (e.g. sustained or permanent displacement of populations).

The ground-based monitoring of volcanic activity, on a real-time basis, is a challenging task, as the instrumentation may be vulnerable to destruction or difficult to manage in remote locations. The present work wants to explore the added value of using geostationary data to follow the entire evolution of volcanic eruptions, expanding monitoring capabilities on an hourly basis. The capability to monitor the area of a volcano every 15 minutes, by using the FRP product from SEVIRI/MSG, allows the identification of the moment of greatest volcanic activity, in near real-time. Despite the lower spatial resolution, the very high temporal resolution and low timeliness may represent a great advantage in comparison with polar satellite products that collect only two observations a day. It should be noted that this added value has been revealed to be higher at low to moderate latitudes where the accuracy of the FRP product is higher [29].

The adopted rationale relies on the fact that Fire Radiative Energy (FRE) released is proportional to the amount of the intensity during Mount Etna and Cumbre Vieja 2021 eruptions, based on the accumulated FRP released by each event [41,42]. ~~The use of FRP as a management tool profits from the accumulated experience of using it to monitor wild-fires.~~ Among the several advantages of using the product, the high sensitivity that allows for detecting sub-pixel fires and the high temporal resolution (15 minutes) allow the continuous monitoring of volcanic activity, being possible to follow up the rapid behavior and direction of the lava flow almost in near real-time.

Considering that FRE is the emitted radiant energy released during combustion, linked to smoke production (49), the possibility to use it as a proxy of volcanic emissions into the atmosphere was also assessed. The very good results of the evaluation of the volcanic activity from Mount Etna and Cumbre Vieja events, show that FRP products can be a valuable proxy of volcanic activity. The released SO_2 concentrations during both eruptions are as well in line with the emitted FRE values, corroborating the hypothesis that FRE can be used as a proxy of volcanic emissions into the atmosphere. Furthermore, it can be concluded that FRP products allow hazard assessment, eruption forecasting and warnings, and risk mitigation during unrest periods to enhance public safety and reduce losses from volcanic events.

Author Contributions: Conceptualization, C.A C.M.G and R.D.; writing—original draft preparation, C.A.; review and editing, R.D.; visualization, C.A., supervision, C.M.G.; All authors have read and agreed to the published version of the manuscript.

Funding: This study was performed within the framework of the LSA-SAF, co-funded by EUMETSAT.

Data Availability Statement: Not applicable

Acknowledgments: Not applicable.

Conflicts of Interest: The authors declare no conflict of interest.

References

1. United Nations Office for Disaster Risk Reduction (2022). Global Assessment Report on Disaster Risk Reduction 2022: Our World at Risk: Transforming Governance for a Resilient Future. Geneva.
2. Caricchi, Luca, et al. "The build-up and triggers of volcanic eruptions." Nature Reviews Earth & Environment 2.7 (2021): 458-476.
3. Understanding Volcano Hazards and Preventing Volcanic Disasters A Science Strategy for the Volcano Hazards Program, U.S. Geological Survey, 2004-2008
4. Corradini, S.; Guerrieri, L.; Stelitano, D.; Salerno, G.; Scollo, S.; Merucci, L.; Prestifilippo, M.; Musacchio, M.; Silvestri, M.; Lombardo, V.; Caltabiano, T. Near Real-Time Monitoring of the Christmas 2018 Etna Eruption Using SEVIRI and Products Validation. Remote Sens. 2020, 12, 1336. https://doi.org/10.3390/rs12081336
5. Lorenzo Guerrieri, Luca Merucci, Stefano Corradini, Sergio Pugnaghi, Evolution of the 2011 Mt. Etna ash and SO2 lava fountain episodes using SEVIRI data and VPR retrieval approach, Journal of Volcanology and Geothermal Research, 291, 2015, 63-71,
6. Andronico, D., Lodato, L., 2005. Effusive Activity at Mount Etna Volcano (Italy) During the 20th Century: A Contribution to Volcanic Hazard Assessment. Natural Hazards 36, 407–443. https://doi.org/10.1007/s11069-005-1938-2.
7. Grainger, R.G.; Highwood, E.J. Changes in stratospheric composition chemistry, radiation and climate caused by volcanic eruptions. In Volcanic Degassing; Geological Society: London, UK, 2003; Volume 213, pp. 329–347. [Google Scholar]
8. V. Salgueiro, J.L. Guerrero-Rascado, M.J. Costa, R. Román, A. Cazorla, A. Serrano, F. Molero, M. Sicard, C. Córdoba-Jabonero, D. Bortoli, A. Comerón, F.T. Couto, M.Á. López-Cayuela, D. Pérez-Ramírez, M. Potes, J.A. Muñiz-Rosado, M.A. Obregón, R. Barragán, D.C.F.S. Oliveira, J. Abril-Gago, R. González, C. Gíl-Díaz, I. Foyo-Moreno, C. Muñoz-Porcar, M.J. Granados-Muñoz, A. Rodríguez-Gómez, M. Herreras-Giralda, J.A. Bravo-Aranda, C.V. Carvajal-Pérez, A. Barreto, L. Alados-Arboledas, Characterization of Tajo gaite volcanic plumes detected over the Iberian Peninsula from a set of satellite and ground-based remote sensing instrumentation, Remote Sensing of Environment, 295, 2023, https://doi.org/10.1016/j.rse.2023.113684.
9. Minnis, P., Harrison, E.F., Stowe, L.L., Gibson, G.G., Denn, F.M., Doelling, D.R., Smith, W.L., 1993. Radiative climate forcing by the mount pinatubo eruption. Science 259, 1411–1415. https://doi.org/10.1126/science.259.5100.1411.
10. Mill´an, L., Santee, M.L., Lambert, A., Livesey, N.J., Werner, F., Schwartz, M.J., Pumphrey, H.C., Manney, G.L., Wang, Y., Su, H., Wu, L., Read, W.G., Froidevaux, L.,2022. The hunga Tonga-hunga ha ' apai hydration of the stratosphere. Geophys. Res. Lett. 49, 1–16. https://doi.org/10.1029/2022GL099381
11. Graf, H. Ä., J. Feichter, and B. R. Langmann (1997), Volcanic sulfur emissions: Estimates of source strength and its contribution to the global sulfate distribution, J. Geophys. Res., 102(D9), 10,727–10,738, https://doi:10.1029/96JD03265.
12. Takebayashi, M., Onishi, M., & Iguchi, M. (2021). Large volcanic eruptions and their influence on air transport: The case of Japan. Journal of Air Transport Management, 97, 102136. https://doi:10.1016/j.jairtraman.2021.102
13. Krotkov, N. A., M. R. Schoeberl, G. A. Morris, S. Carn, and K. Yang (2010), Dispersion and lifetime of the SO2 cloud from the August 2008 Kasatochi eruption, J. Geophys. Res., 115, D00L20, https://doi:10.1029/2010JD013984.
14. Wang, J., S. Park, J. Zeng, C. Ge, K. Yang, S. Carn, N. Krotkov, and A. H. Omar (2013), Modeling of 2008 Kasatochi volcanic sulfate direct radiative forcing: Assimilation of OMI SO2 injection altitude data and comparison with MODIS and CALIOP observations, Atmos. Chem. Phys., 13, 1895–1912, https://doi:10.5194/acp-13-1895-2013.
15. Hansell A, Oppenheimer C. Health hazards from volcanic gases: a systematic literature review. Arch Environ Health. 2004 Dec; 59 (12):628-39. https://doi: 10.1080/00039890409602947. PMID: 16789471.
16. Manisalidis I, Stavropoulou E, Stavropoulos A and Bezirtzoglou E (2020) Environmental and Health Impacts of Air Pollution: A Review. Front. Public Health 8:14. https://doi: 10.3389/fpubh.2020.00014
17. Pavlidou, E., Hecker, C., van der Werff, H.,& van der Meijde, M. (2017). Study of volcanic activity at different time scales using hypertemporal land surface temperature data. Journal of Geophysical Research: Solid Earth, 122, 7613–7625. https://doi.org/10.1002/2017JB014317
18. Coppola D, Laiolo M, Cigolini C, Massimetti F, Delle Donne D, Ripepe M, Arias H, Barsotti S, Parra CB, Centeno RG, Cevuard S, Chigna G, Chun C, Garaebiti E,Gonzales D, Griswold J, Juarez J,Lara LE, López CM, Macedo O,Mahinda C, Ogburn S, Prambada O,Ramon P, Ramos D, Peltier A,Saunders S, de Zeeuw-van Dalfsen E,Varley N and William R (2020) Thermal Remote

Sensing for Global Volcano Monitoring: Experiences From the MIROVA System. Front. Earth Sci. 7:362. https://doi: 10.3389/feart.2019.00362

19. Corradini, S.; Montopoli, M.; Guerrieri, L.; Ricci, M.; Scollo, S.; Merucci, L.; Marzano, F.S.; Pugnaghi, S.; Prestifilippo, M.; Ventress, L.J.; et al. Multi-Sensor Approach for Volcanic Ash Cloud Retrieval and Eruption Characterization: The 23 November 2013 Etna Lava Fountain. Remote Sens. 2016, 8, 58.
20. Corradini, S.; Guerrieri, L.; Lombardo, V.; Merucci, L.; Musacchio, M.P.; Estifilippo, M.; Scollo, S.; Silvestri, M.; Spata, G.; Stelitano, D. Proximal monitoring of the 2011–2015 Etna lava fountains using MSG-SEVIRI data. Geosciences 2018, 8, 140.
21. Global Assessment Report on Disaster Risk Reduction 2014,a
22. Barberi, F., Carapezza, M.L., Valenza, M., Villari, L., 1993. The control of lava flow during the 1991–1992 eruption of Mt. Etna. Journal of volcanology and geothermal research 56 (1–2), 1–34.
23. Harris, A.J.L., Steffke, A., Calvari, S., Spampinato, L., 2011. Thirty years of satellite-derived lava discharge rates at Etna: Implications for steady volumetric output. J. Geophys. Res. 116, B08204. https://doi.org/10.1029/2011JB008237
24. Proietti, C., Coltelli, M., Marsella, M., Martino, M., Scifoni, S., Giannone, F., 2020. Towards a satellite-based approach to measure eruptive volumes at Mt. Etna using Pleiades datasets. Bulletin of Volcanology 82 (4), 1–15.
25. Marina Bisson, Claudia Spinetti, Daniele Andronico, Monica Palaseanu-Lovejoy, Maria Fabrizia Buongiorno, Oleg Alexandrov, Thomas Cecere, Ten years of volcanic activity at Mt Etna: High-resolution mapping and accurate quantification of the morphological changes by Pleiades and Lidar data, International Journal of Applied Earth Observation and Geoinformation,Volume 102,2021,102369, ISSN 0303-2434, https://doi.org/10.1016/j.jag.2021.102369.
26. LONGPRÉ, MARC-ANTOINE,2021. Reactivation of Cumbre Vieja volcano, Vol 374, Issue 6572 • pp. 1197-1198 • DOI: 10.1126/science.abm9423
27. Smith, A.M.S.; Wooster, M.J. Remote classification of head and backfire types from MODIS fire radiative power and smoke plume observations. Int. J. Wildland Fire 2005, 14, 249–254.
28. Johnston, J.M.; Wooster, M.J.; Paugam, R.; Wang, X.; Lynham, T.J.; Johnston, L.M. Direct estimation of Byram's fire intensity from infrared remote sensing imagery. Int. J. Wildland Fire 2017, 26, 668–684
29. Wooster et al.,2015, LSA SAF Meteosat FRP products-Part 1: Algorithms, product contents, and analysis. Atmospheric Chemistry and Physics, 15(22), 13217-13239.]
30. Stothers, R. B., & Rampino, M. R. (1983). Historic volcanism, European dry fogs, and Greenland acid precipitation, 1500 BC to AD 1500. *Science*, *222*(4622), 411-413
31. Calvari, S., & Nunnari, G. (2022). Etna Output Rate during the Last Decade (2011–2022): Insights for Hazard Assessment. *Remote Sensing*, *14*(23), 6183.
32. Branca, S., Del Carlo, P., 2004. Eruptions of Mt Etna during the past 3.200 years: a revised compilation integrating the Historical and stratigraphic records. Mt. volcano laboratory. AGU, Etna
33. Andronico, D., Lodato, L., 2005. Effusive Activity at Mount Etna Volcano (Italy) During the 20th Century: A Contribution to Volcanic Hazard Assessment. Natural Hazards 36, 407–443. https://doi.org/10.1007/s11069-005-1938-2.
34. LSA SAF. Fire Radiative Power; Validation Report; LSA SAF: Lisbon, Portugal, 2015.
35. Govaerts, Y.M. Wooster, Roberts, G., Freeborn, P., XU, W., He, J. and Lattanzio A (2015) MSG SEVIRI Fire Radiative Power (FRP) characterization Algorithm Theoretical Basis Document Version 2.8 , Report No EUM/MET/SPE/06/0398, 2015
36. Philpotts, Anthony R.; Ague, Jay J. (2022). Principles of igneous and metamorphic petrology (32nd ed.). Cambridge, UK: Cambridge University Press. pp. 35, DOI: 10.1017/9781108631419
37. C. Archambault, J.C. Tanguy, Comparative temperature measurements on mount etna lavas: problems and techniques, Journal of Volcanology and Geothermal Research, Volume 1, Issue 2, 1976, Pages 113-125, ISSN 0377-0273, https://doi.org/10.1016/0377-0273(76)90002-0.
38. Klügel, A., Hansteen, T. H., & Galipp, K. (2005). Magma storage and underplating beneath Cumbre Vieja volcano, La Palma (Canary Islands). Earth and Planetary Science Letters, 236(1-2), 211–226. doi:10.1016/j.epsl.2005.04.006
39. Pinto, Miguel & Dacamara, Carlos & Trigo, Isabel & Trigo, Ricardo & Turkman, K.. (2018). Fire danger rating over Mediterranean Europe based on fire radiative power derived from Meteosat. Natural Hazards and Earth System Sciences Discussions. 1-23. 10.5194/nhess-2017-346.
40. Durão, Rita, Catarina Alonso, and Célia Gouveia. "The Performance of ECMWF Ensemble Prediction System for European Extreme Fires: Portugal/Monchique in 2018." Atmosphere 13.8 (2022): 1239.
41. Durand M, Grattan J. Effects of volcanic air pollution on health. Lancet 2001 ; 357:164
42. CAMS, 2021. https://atmosphere.copernicus.eu/cams-monitors-transport-so2-la-palma-volcano
43. Global Volcanism Program, 2021. Report on Etna (Italy) (Bennis, K.L., and Venzke, E., eds.). Bulletin of the Global Volcanism Network, 46:4. Smithsonian Institution.
44. Global Volcanism Program, 2021. Report on Etna (Italy). In: Sennert, S K (ed.), Weekly Volcanic Activity Report, 17 February-23 February 2021. Smithsonian Institution and US Geological Survey.
45. Global Volcanism Program, 2021. Report on Etna (Italy). In: Sennert, S K (ed.), Weekly Volcanic Activity Report, 30 June-6 July 2021. Smithsonian Institution and US Geological Survey.

46. Global Volcanism Program, 2021. Report on La Palma (Spain) (Crafford, A.E., and Venzke, E., eds.). Bulletin of the Global Volcanism Network, 46:10. Smithsonian Institution. https://doi.org/10.5479/si.GVP.BGVN202110-383010
47. Wooster, M.J.; Roberts, G.; Perry, G.; Kaufman, Y. Retrieval of biomass combustion rates and totals from fire radiative power observations: FRP derivation and calibration relationships between biomass consumption and fire radiative energy release. J. Geophys. 405 Res. Atmos. 2005, 110, 2005
48. Directive 2008/50/EC of the European Parliament and of the Council of 21 May 2008 on ambient air quality and cleaner air for Europe, OJ L 152, 11.6.2008, p. 1–44 (BG, ES, CS, DA, DE, ET, EL, EN, FR, IT, LV, LT, HU, MT, NL, PL, PT, RO, SK, SL, FI, SV), Special edition in Croatian: Chapter 15 Volume 029 P. 169 – 212